



**HAL**  
open science

## SEI Composition on Hard Carbon in Na-Ion Batteries After Long Cycling: Influence of Salts (NaPF<sub>6</sub>, NaTFSI) and Additives (FEC, DMCF)

J. Fondard, E. Irisarri, Cecile Courreges, M. Palacin, A. Ponrouch, Rémi  
Dedryvère

### ► To cite this version:

J. Fondard, E. Irisarri, Cecile Courreges, M. Palacin, A. Ponrouch, et al.. SEI Composition on Hard Carbon in Na-Ion Batteries After Long Cycling: Influence of Salts (NaPF<sub>6</sub>, NaTFSI) and Additives (FEC, DMCF). *Journal of The Electrochemical Society*, 2020, Challenges in Novel Electrolytes, Organic Materials, and Innovative Chemistries for Batteries in Honor of Michel Armand, 167 (7), pp.070526. 10.1149/1945-7111/ab75fd . hal-02534879

**HAL Id: hal-02534879**

**<https://hal.science/hal-02534879v1>**

Submitted on 2 Oct 2020

**HAL** is a multi-disciplinary open access archive for the deposit and dissemination of scientific research documents, whether they are published or not. The documents may come from teaching and research institutions in France or abroad, or from public or private research centers.

L'archive ouverte pluridisciplinaire **HAL**, est destinée au dépôt et à la diffusion de documents scientifiques de niveau recherche, publiés ou non, émanant des établissements d'enseignement et de recherche français ou étrangers, des laboratoires publics ou privés.

**OPEN ACCESS**

## SEI Composition on Hard Carbon in Na-Ion Batteries After Long Cycling: Influence of Salts ( $\text{NaPF}_6$ , NaTFSI) and Additives (FEC, DMCF)

To cite this article: J. Fondard *et al* 2020 *J. Electrochem. Soc.* **167** 070526

View the [article online](#) for updates and enhancements.



The banner features a background image of Earth from space. On the left, there are three circular logos: the ECS logo, the Electrochemical Society logo, and the Korean Electrochemical Society logo. The central text reads: "Joint International Meeting PRiME 2020 October 4-9, 2020". Below this, a blue bar contains the text "Attendees register at NO COST!". On the right side, there is a large logo for "PRiME PACIFIC RIM MEETING ON ELECTROCHEMICAL AND SOLID STATE SCIENCE 2020". At the bottom right, a blue button with white text says "REGISTER NOW" with a right-pointing arrow.



# SEI Composition on Hard Carbon in Na-Ion Batteries After Long Cycling: Influence of Salts (NaPF<sub>6</sub>, NaTFSI) and Additives (FEC, DMCF)

J. Fondard,<sup>1,=</sup> E. Irisarri,<sup>2,=</sup> C. Courrèges,<sup>1,3,4</sup> M. R. Palacin,<sup>2,4,\*</sup> A. Ponrouch,<sup>2,4,\*</sup> and R. Dedryvère<sup>1,3,4,z</sup>

<sup>1</sup>IPREM, CNRS, Université de Pau & Pays Adour, E2S-UPPA, Hélioparc, 64053 Pau Cedex 9, France

<sup>2</sup>Institut de Ciència de Materials de Barcelona (ICMAB-CSIC), Campus UAB, E-08193 Bellaterra, Catalonia, Spain

<sup>3</sup>Réseau sur le Stockage Electrochimique de l'Energie (RS2E), CNRS FR 3459, France

<sup>4</sup>ALISTORE-ERI, European Research Institute

A study of the Solid Electrolyte Interphase (SEI) on hard-carbon (HC) electrodes in sodium half-cells is presented. Electrochemical performances over > 100 cycles were compared with two different salts (NaPF<sub>6</sub>, NaTFSI) and two different electrolyte additives (FEC, DMCF) in a mixture of EC and DMC solvents. The best electrochemical performances were observed with NaPF<sub>6</sub> salt in conjunction with 3% FEC. The DMCF additive had a detrimental effect in all electrolyte combinations. The chemical characterization of the SEI was carried out by X-ray Photoelectron Spectroscopy (XPS) and showed that the best electrochemical behavior was related to an SEI composition based on sodium ethylene dicarbonate and NaF, whereas poorer electrochemical performances were associated to either low NaF or high Na<sub>2</sub>CO<sub>3</sub> content. The results reported herein provide an insight on the SEI chemistry on hard carbon electrodes in sodium cells after long-term cycling, as a complement to previous studies dealing with the first cycles.

© 2020 The Author(s). Published on behalf of The Electrochemical Society by IOP Publishing Limited. This is an open access article distributed under the terms of the Creative Commons Attribution Non-Commercial No Derivatives 4.0 License (CC BY-NC-ND, <http://creativecommons.org/licenses/by-nc-nd/4.0/>), which permits non-commercial reuse, distribution, and reproduction in any medium, provided the original work is not changed in any way and is properly cited. For permission for commercial reuse, please email: [oa@electrochem.org](mailto:oa@electrochem.org). [DOI: 10.1149/1945-7111/ab75fd]



Manuscript submitted December 31, 2019; revised manuscript received February 5, 2020. Published February 24, 2020. *This paper is part of the JES Focus Issue on Challenges in Novel Electrolytes, Organic Materials, and Innovative Chemistries for Batteries in Honor of Michel Armand.*

Supplementary material for this article is available [online](#)

Sodium-ion batteries (SIBs) are re-attracting the interest of the scientific community in the last years due to speculations about potential supply risk for lithium related to expanding the field of applications for Lithium-ion batteries (LIBs) from portable electronics to transportation and electricity sectors.<sup>1</sup> Time will tell whether such risk is merely related to consumption-production temporary imbalance or else it may have long-term implications. Yet, diversification of battery technologies seems a wise strategy to pursue considering that different applications have clearly different requirements in terms of cost, performance and sustainability. Progress in SIBs is catalyzed by the chemical analogies between lithium and sodium,<sup>2,3</sup> and start-ups such as Faradion (UK) and Tiamat (France) are already producing cells, and available cost and resource analysis do offer interesting perspectives for the future.<sup>4-6</sup> Moreover, no significant modification of the battery production line is expected when moving from Li-ion to Na-ion batteries. In the last years, research efforts were focused on finding the best electrodes/electrolyte combination. While on the negative side, Hard Carbon (HC) seems to be the only practically viable material at this stage,<sup>7</sup> both polyanionic and layered electrode materials are considered on the positive side.<sup>8</sup> In line with the progress in LIBs, the role of the electrolyte has at a first sight been deemed less relevant. Yet, electrolyte formulation is crucial for practical performance.<sup>9</sup> Beyond intrinsic features, the quality and stability of the Solid Electrolyte Interphase (SEI) is crucial to cycle life, and also, indirectly, to the overall cell service life cost.<sup>10,11</sup> The cathodic stability of an electrolyte depends on its Lowest Unoccupied Molecular Orbital (LUMO) level. If only thermodynamics is considered, the electrolyte component with the lowest LUMO level will be reduced first in contact with the HC electrode, possibly contributing to the formation of the SEI. Therefore, the electrolyte's formulation dictates the SEI

composition and its properties such ionic conductivity, electronic resistance, stability, thickness, etc. Moreover, despite having been intensively studied,<sup>12,13</sup> full understanding of the SEI is still elusive in LIBs, as its nature is highly dependent on electrolyte composition (including additives) and can dynamically evolve depending on cell operation conditions, time and temperature.<sup>14</sup>

In the case of SIBs, the understanding is still in a more preliminary stage.<sup>15</sup> The most commonly used electrolytes consist of a solution of NaPF<sub>6</sub> (typically 1 mol l<sup>-1</sup>) in a mixture of alkyl carbonate based solvents such as dimethyl carbonate (DMC), Diethyl carbonate (DEC), Ethyl carbonate (EC) or Propylene Carbonate (PC). Beyond the expected analogies between LIBs and SIBs as a result of this chemical analogy, some relevant differences (e.g. the solubility of SEI components<sup>11,16</sup> or its mechanical properties<sup>17</sup>) that can be critical for performance were early realized. M. Armand and co-workers were pioneers in the systematic investigation of the effect of salt anions in the SEI formed on hard carbon upon first reduction using different mixtures of alkyl carbonates as solvents, which largely influences coulombic efficiency on the first cycle and hence the practical energy density of the full cell.<sup>18</sup> They found that the main components of the SEI are double alkylcarbonates, with linear solvent molecules exhibiting higher reactivity towards hard carbon electrodes, and onset thermal stability for a given solvent being highly dependent, on the salt, in agreement with previous findings.<sup>19</sup>

In parallel, Lucht et al.<sup>20</sup> studied the SEI on hard carbon after 25 cycles in 1 M NaPF<sub>6</sub> in EC/DEC at 18 mA h<sup>-1</sup> (equivalent to C/20 arbitrarily considering a theoretical capacity of 372 mAh g<sup>-1</sup> corresponding to graphite in LIBs) and were able to conclude that it was mostly consisting of sodium ethylene dicarbonate (NEDC), derived from EC reduction, and NaF, similarly to what was found on LIBs. Again, some more subtle differences exist beyond this apparent similarity at first sight. Komaba et al.<sup>21</sup> were the first to test the effect in NIBs of conventional electrolyte additives used in LIBs and found that while difluoroethylene carbonate (DFEC) and vinylene carbonate (VC) did not improve cycle life for 1 M NaClO<sub>4</sub>

<sup>=</sup>These authors contributed equally to this work.

\*Electrochemical Society Member.

<sup>z</sup>E-mail: [aponrouch@icmab.es](mailto:aponrouch@icmab.es); [remi.dedryvere@univ-pau.fr](mailto:remi.dedryvere@univ-pau.fr)

in PC electrolyte, the presence of fluoroethylene carbonate (FEC) was beneficial. Extension of the study to  $\text{NaPF}_6$  based electrolytes showed further improvement, which was attributed to some sort of synergistic effect,<sup>22,23</sup> with atomistic reaction simulations indicating the existence of an optimum value for FEC concentration in the electrolyte, beyond which it would have detrimental effects.<sup>24</sup> In contrast, some detrimental effects of FEC were also reported, such as an increase in polarization in two-electrode cell associated with a more resistive SEI layer formed on the Na metal counter electrode.<sup>25,26</sup>

Since the origin of polarization cannot be clearly assessed in tests carried out in two electrode cells, in the present paper we decided to embark in a comparative study using EC:DMC based electrolytes (which typically exhibit low viscosity and hence good wettability of the separator) and two different salts:  $\text{NaPF}_6$  and  $\text{NaTFSI}$ , the main advantages of the latter being low toxicity, improved safety and higher stability in presence of trace water and the main concern being corrosion of aluminum in  $\text{TFSI}^-$  anions containing liquid electrolytes.<sup>27</sup> We have also tested the effect of FEC as additive in two different concentrations, and we have carried out a comparative study with fluorinated dimethylcarbonate (DMCF) as alternative additive.

Specific efforts were done to probe the influence of the salt and additive nature on electrochemical performances and SEI composition after long-term cycling. Cells were cycled in EC:DMC (1:1 vol.) mixture of solvents with  $\text{NaPF}_6$  and  $\text{NaTFSI}$  salts, with 1.5–3 wt% of FEC or DMCF additive. HC//Na half-cells were cycled from 0.003 V to 2 V for 135 cycles at 0.1 C and the evolution of the SEI composition was followed by X-ray Photoelectron Spectroscopy (XPS).

### Experimental

Composite electrodes containing hard carbon (HC) as active material were prepared from N-Methylpyrrolidone based slurries. Their compositions were 92 wt% HC, 3 wt% carbon black (Super P

Timcal) and 5 wt% PVdF (polyvinylidene fluoride, with a loading of  $2.5 \text{ mg HC cm}^{-2}$ ). Commercial HC was used with surface area below  $10 \text{ m}^2 \text{ g}^{-1}$  as measured by means of Brunauer–Emmett–Teller (BET) using an ASAP 2000 Micromeritics Instrument. Electrochemical cycling of HC was performed in three-electrode Swagelok cells with sodium metal as reference and counter electrodes in order to avoid any significant potential shift of the reference electrode upon cycling.<sup>16</sup> Cycling was carried out in galvanostatic mode with potential limitation (GCPL) at different rates using a Bio-Logic VMP3 potentiostat. Glass borosilicate fiber was used as separator soaked in  $150 \mu\text{l}$  of electrolyte. The electrolytes consist of 1 M  $\text{NaPF}_6$  or 1 M  $\text{NaTFSI}$  in a 1:1 mixture of ethylene carbonate (EC) and dimethyl carbonate (DMC), with or without 1.5 or 3 wt% FEC or DMCF additives. The water content in all electrolytes was measured by Karl-fisher titration and found to be lower than 20 ppm in all cases.

The composition of the SEI was investigated by XPS on HC electrodes recovered from cells immediately after cycling. The cells were open inside an Ar-filled glove box, and each electrode was cut in two halves, one of which was soaked in three successive dimethyl carbonate (DMC) baths while the other one and the separator were kept without further treatment for comparison.

X-ray Photoelectron Spectroscopy (XPS) was carried out with a Thermo Scientific Escalab 250 Xi spectrometer using a focused monochromatized radiation at two different photon energies: Al  $K\alpha$  ( $h\nu = 1486.6 \text{ eV}$ ) and Ag  $L\alpha$  ( $h\nu = 2984.2 \text{ eV}$ ). The analyzed area of the samples was a  $450 \times 900 \mu\text{m}^2$  ellipse. Peaks were recorded with a constant pass energy of 20 eV. The binding energy scale was calibrated from the hydrocarbon contamination using the C 1s peak at 285.0 eV. For all analyses, thorough precautions were taken to preserve the samples surface from any contact with air and moisture. All samples were handled or stored in controlled dry argon atmosphere. The XPS transfer chamber was directly connected to the argon glovebox. No argon ion sputtering was used to etch the samples surface for depth-profiling, in order to avoid any ion beam-induced chemical changes leading to wrong conclusions. Instead, the

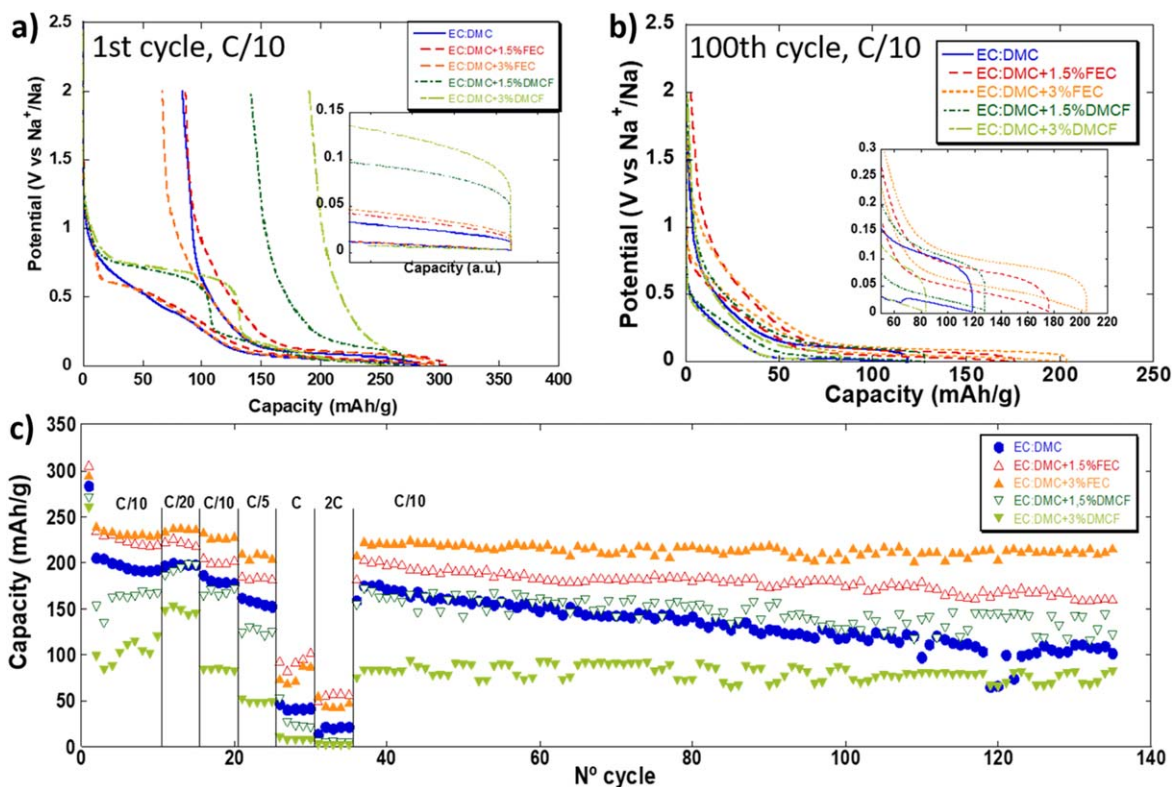


**Figure 1.** Potential vs capacity profile for the 1st and 100th cycle and capacity vs cycle number for HC electrodes cycled at different successive galvanostatic rates in three electrode cells using 1 M  $\text{NaPF}_6$  in EC:DMC with addition of 1.5 and 3% of FEC or DMCF.

two photon energies were used to get access to two different probe depths. As it was mentioned in previous papers that the SEI layer components in Na-ion batteries may be more soluble in the electrolyte than in Li-ion batteries,<sup>11,16</sup> we evaluated the effect of the washing process of the HC electrodes by DMC prior to surface characterization by XPS. The HC electrodes were washed by  $3 \times 1$  min immersion in pure anhydrous DMC baths to get rid of the electrolyte. DMC was then evaporated by leaving the electrode under vacuum (inside the glovebox antechamber) for at least 1 h. As no significant differences were observed related to the carbonaceous species present in the SEI, it was decided to show only the results obtained on washed samples. Nonetheless, a comparison between washed and unwashed electrodes can be drawn from the example of a HC electrode cycled using a NaTFSI-based electrolyte given as supplementary information (Fig. S1 is available online at [stacks.iop.org/JES/167/070526/mmedia](https://stacks.iop.org/JES/167/070526/mmedia)).

## Results and Discussion

**Electrochemical performances.**—Capacity evolution upon cycle number for HC electrodes was monitored in three-electrode half cells cycled in galvanostatic mode with potential limitation (GCPL) with 0.003 V and 2 V as low and high cut off voltages, respectively, at different successive rates C/10, C/20, C/5, C, 2 C and further cycling at C/10 (considering  $372 \text{ mAh g}^{-1}$  as theoretical capacity). Results obtained using  $\text{NaPF}_6$  based electrolyte with or without additive (FEC or DMCF) are presented in Fig. 1. In additive-free electrolyte, the electrochemical profile for the first cycle exhibits two regions, an almost linear potential decay centered around 0.5 V vs  $\text{Na}^+/\text{Na}$  and a pseudo plateau around 0.1 V  $\text{Na}^+/\text{Na}$ . While the complete understanding of the redox/capacitive processes at play in this system is still lacking,<sup>28,29</sup> such GCPL curves are well known and typical for HC electrodes.

The presence of additive in the electrolyte significantly impacts the electrochemical curves. When DMCF is added, an additional reduction pseudo plateau can be seen at ca. 0.75 V vs  $\text{Na}^+/\text{Na}$ . The

length of such plateau appears to be related to the amount of DMCF initially present in solution (Fig. 1a). Indeed, the capacity associated with this plateau correspond to about 39 or 50% of the total capacity recorded upon the first reduction when 1.5 or 3% of DMCF is used, respectively. This pseudo plateau disappears upon further cycling (Fig. 1b) evidencing the irreversibility of the redox process involved. Much lower first cycle coulombic efficiencies are recorded in presence of DMCF (ca. 70% in additive free electrolyte and 48% and 27% with 1.5% and 3% of DMCF, respectively). When FEC is added, the linear potential decay upon the first reduction partially disappeared and a reduction pseudoplateau can be seen at ca. 0.55 V vs  $\text{Na}^+/\text{Na}$ . As for DMCF, such pseudo plateau is no longer visible after the first cycle (Fig. 1b). By contrast with DMCF, the addition of FEC resulted in a slight improvement of the first cycle coulombic efficiency. Indeed, 70% first cycle coulombic efficiency was recorded in additive free electrolyte and 72% and 77% with 1.5 and 3% of FEC, respectively. In terms of overall capacity of the HC electrode (Fig. 1c) the addition of DMCF and FEC have radically different impact. While the presence of DMCF is detrimental (with about 200, 150 and  $100 \text{ mAh g}^{-1}$  recorded in electrolyte with 0%, 1.5% or 3% DMCF, respectively) the addition of FEC improves the reversible capacity as well as the capacity retention upon cycling. Indeed, capacities of about 200, 220 and  $230 \text{ mAh g}^{-1}$  were recorded in electrolyte with 0%, 1.5% or 3% FEC, respectively (at C/10 and for cycle number 10) and 65%, 72% and 94% capacity retention was measured after 130 cycles with 0%, 1.5% or 3% FEC, respectively. The difference in the reversible capacity recorded with and without FEC or DMCF can be rationalized by comparing the overpotential between charge and discharge (see onsets in Figs. 1a and 1b). Indeed, during the first cycle, this overpotential is the highest ( $> 60 \text{ mV}$ ) when DMCF is present in the electrolyte resulting in partial loss of capacity associated with the low voltage pseudo plateau.<sup>30</sup> Upon cycling, the overpotential in additive free electrolyte significantly increase from less than 20 mV during the first cycle up to about 60 mV after 100 cycles resulting in low

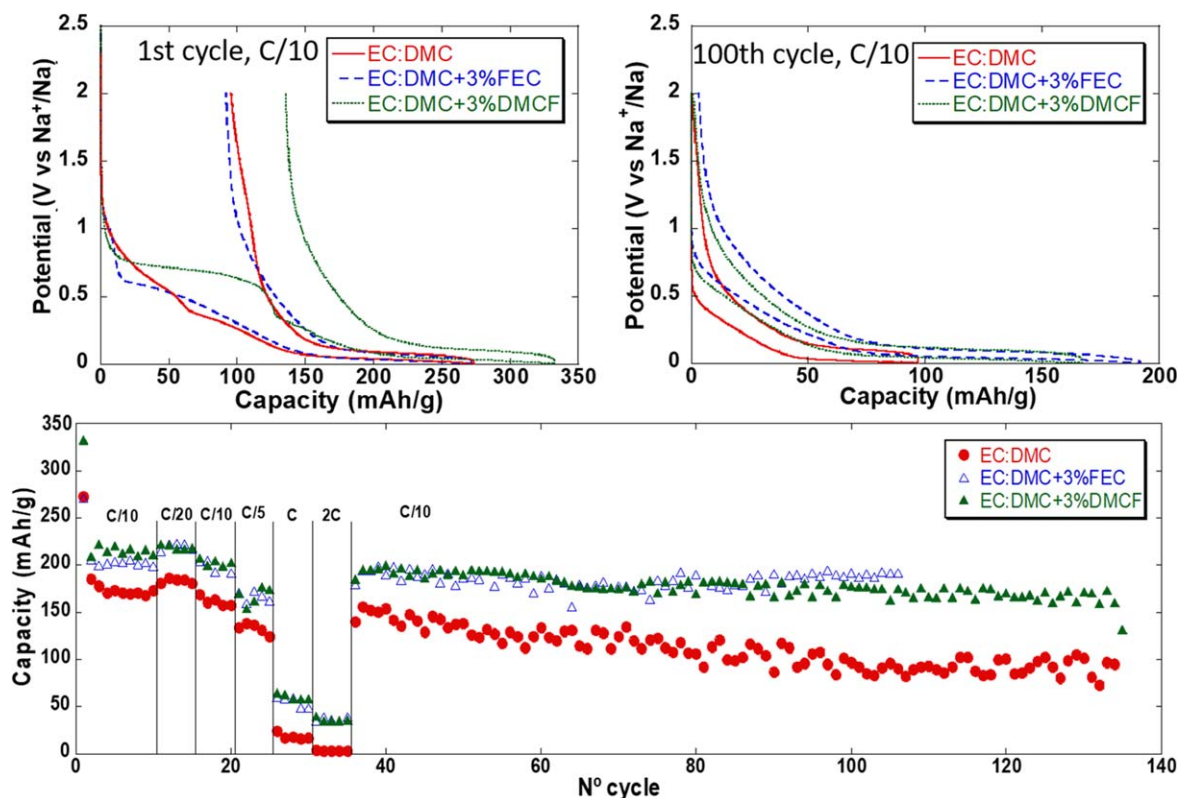


**Figure 2.** Potential vs capacity profile for the 1st and 100th cycle and capacity vs cycle number for HC electrodes (Tape 1) cycled at different successive galvanostatic rates in three electrode cells using 1 M NaTFSI in EC:DMC with addition of 3% of FEC or DMCF.

capacity retention. The overpotential was however found to remain stable both with FEC or DMCF additives, resulting in better capacity retention upon cycling. In all cases, coulombic efficiency values of about 99% are recorded after a conditioning period of 10 to 20 cycles.

Moving to NaTFSI based electrolytes (Fig. 2), the trends explained above for NaPF<sub>6</sub> based electrolytes only partially hold. For instance, addition of DMCF or FEC also lead to the appearance during the first reduction of an irreversible pseudo plateau at ca. 0.75 or 0.55 V vs Na<sup>+</sup>/Na, respectively. Lower first cycle coulombic efficiencies were measured with DMCF containing electrolytes than with or without FEC. However, in NaTFSI based electrolytes the addition of FEC or DMCF was found to be beneficial in terms of overall capacity and capacity retention upon cycling (Fig. 2c). This is in stark contrast with the NaPF<sub>6</sub> based system in which the addition of DMCF was clearly detrimental to the overall capacity recorded.

**Chemical characterization of the SEI.—Cycling with NaPF<sub>6</sub> salt and FEC additive.**—Figure 3 shows C 1s and F 1s XPS spectra of HC electrodes after 135 cycles in half-cells with NaPF<sub>6</sub>/EC:DMC electrolyte, without and with 3% FEC. Figures depicting other spectra (O 1s, P 2p and Na 2s) and the quantification of all peaks are given in the SI (Fig. S2 and Table SI). The four C 1s peaks observed in Fig. 3a ( $h\nu = 1486.6$  eV) are characteristic of different carbon environments corresponding to species present in the SEI: (i) 285.0 eV for C atoms bound to only H or other C atoms, corresponding to aliphatic chains and also hydrocarbon surface contamination, as usually observed in XPS spectra, (ii) 286.5–286.7 eV for C atoms bound to one oxygen (yellow component), (iii) 288.3–288.4 eV for O=C=O environments (blue), and finally (iv) 290 eV for carbonate (CO<sub>3</sub>) environments (green). By comparing C 1s spectra obtained without additive and with 3% FEC, it appears that the relative intensity ratios of these components do not significantly change, except for the C–C/C–H component. C 1s spectra with a higher photon energy ( $h\nu = 2984.2$  eV, Fig. 3b) were also recorded in order to increase the probe depth and thus get more information on the volumetric distribution of species in the SEI. The probe depth, defined as three times the photoelectron inelastic mean free path, can be calculated as a function of the photon energy  $h\nu$  using, for instance, TPP-2M model from Tanuma et al.<sup>31</sup> For both reference compounds Na<sub>2</sub>CO<sub>3</sub> and NaF which are frequently found as major constituents in the SEI, the probe depth is about 8–9 nm for  $h\nu = 1486.6$  eV and about 16–17 nm for  $h\nu = 2984.2$  eV, i.e. twice greater. Therefore, these values can be taken as an approximation of

the XPS probe depth for the SEI at these two photon energies. For  $h\nu = 2984.2$  eV in Fig. 3b no significant differences can be observed in C–O, COO and CO<sub>3</sub> relative contributions as compared to  $h\nu = 1486.6$  eV photon energy. Therefore, the SEI composition in these carbon environments can be considered as homogeneous in depth, at least over the first 16–17 nm. The COO environments are certainly related to species coming from the degradation of solvents (EC and DMC) through breaking one C–O bond of the carbonate group, such as R–COONa, as this kind of mechanism was already proposed for Li-ion batteries using the same solvents.<sup>32</sup> The intensity of the C–C/C–H component decreases weakly, indicating that the contribution of hydrocarbon surface contamination to this peak is very small. This is especially true for 3% FEC, for which minor differences are observed for the two photon energies. These findings are consistent with aliphatic chains being present in the SEI, for example in the form of polyolefins, as also suggested for Li-ion batteries with the same kind of solvents.<sup>33</sup> Moreover, the addition of FEC to the electrolyte increases the proportion of aliphatic chains (from 13 to 24 at%). Note that the increase of excitation energy does not lead to enhancement of the very weak component at BE  $\approx 283$  eV. Therefore, this component should not be attributed to HC active material, but should rather be interpreted as a small asymmetry of the peak on the low binding energy (BE) side.

Differences can also be noticed in the F 1s spectra (Fig. 3c). These display the signature of the salt NaPF<sub>6</sub> remaining at the electrode surface (green component, BE  $\approx 687$  eV) and of NaF ensuing from its degradation (red component, BE  $\approx 684$  eV). Intensity differences allow to infer that the amount of NaF is about 10 times greater after cycling with 3% FEC than without additive (5.5 at% instead of 0.5 at%).

XPS valence spectra (Fig. 4) can be used as a fingerprint of the major compounds present at the surface, unless there is a large number of species present in similar amounts, otherwise data interpretation is too complex. In the left part of Fig. 4, the valence spectra of the samples without and with 3% FEC (a and b, respectively) have been compared with those of the reference compounds Na<sub>2</sub>CO<sub>3</sub> and NaF (c and d, respectively). The spectra of the two HC samples present some similarities with the spectrum of Na<sub>2</sub>CO<sub>3</sub>, namely peaks A, C, D, G and H. However, peaks E and F in the 13–20 eV BE region do not seem to be related to Na<sub>2</sub>CO<sub>3</sub>, and comparison with lithium counterparts may be useful to ascertain its origin. The XPS valence spectra of Li<sub>2</sub>CO<sub>3</sub> and lithium alkyl carbonates ROCO<sub>2</sub>Li have similar shapes,<sup>34</sup> as shown in the right part of Fig. 4. Peaks A, C and D are almost identical, with only and the two main following differences: (i) in Li<sub>2</sub>CO<sub>3</sub> (e), the narrow

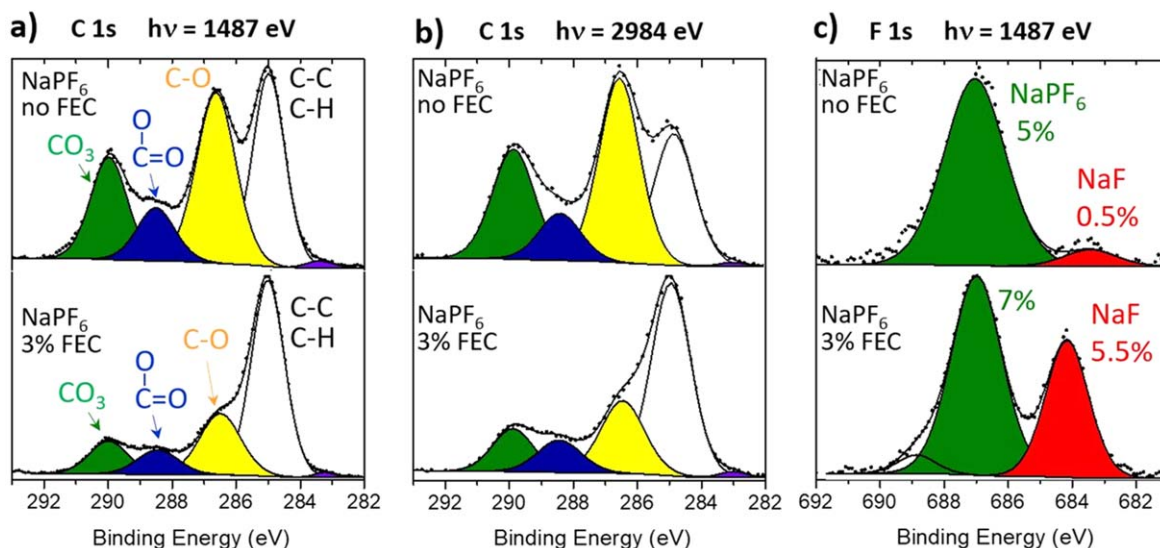


**Figure 3.** (a), (b) C 1s and (c) F 1s XPS spectra of HC electrodes after 135 cycles in half-cells with NaPF<sub>6</sub>/EC:DMC electrolyte, without and with 3% FEC. For C 1s spectra two different photon energies have been used (1487 and 2984 eV, corresponding to different probe depths).

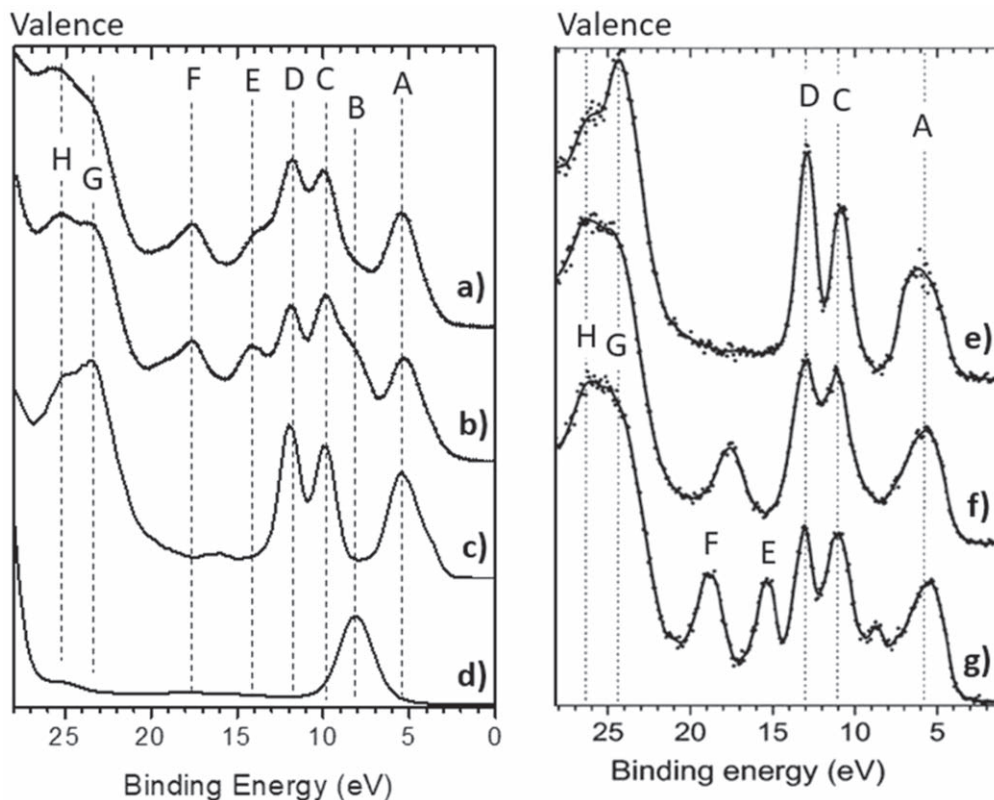


**Figure 4.** XPS valence spectra ( $h\nu = 1487$  eV) of HC electrodes after 135 cycles in half-cells with NaPF<sub>6</sub>/EC:DMC electrolyte: (a) without FEC, (b) with 3% FEC. Comparison with valence spectra of reference compounds recorded in the lab: (c) Na<sub>2</sub>CO<sub>3</sub>, (d) NaF, (e) Li<sub>2</sub>CO<sub>3</sub>, (f) CH<sub>3</sub>OCO<sub>2</sub>Li, (g) CH<sub>3</sub>CH<sub>2</sub>OCO<sub>2</sub>Li. Spectra e, f and g are reproduced from Ref. 31 with permission (Copyright 2005 the American Chemical Society).

peak G is the maximum of the spectrum, while for lithium alkyl carbonates ROCO<sub>2</sub>Li (**f** and **g**), it is reduced to a shoulder on the lower BE side of peak H, and (*ii*) in ROCO<sub>2</sub>Li, additional components are observed in the 13–20 eV BE region, their number being equal to the number of C atoms in the alkyl group R. It was also shown, with the help of *ab initio* calculations, that the contribution of lithium to the valence spectrum is negligible due to the electronic configuration  $ns^0$  of alkaline cations. Therefore, the shape of these spectra seems only governed by the carbon and oxygen backbone of the molecule. This is in perfect agreement with the similarity between the spectra of Na<sub>2</sub>CO<sub>3</sub> and Li<sub>2</sub>CO<sub>3</sub>, as observed in Figs. 4c and 4e, the main difference between the two spectra being a slight shift of Na<sub>2</sub>CO<sub>3</sub> towards lower BE values, due to the higher electropositive character of Na compared to Li. As a result, since we could not record the experimental valence spectra of the reference compounds ROCO<sub>2</sub>Na (their synthesis is indeed rather delicate and they are quite difficult to isolate), we assume we can use the valence spectra of their lithium counterparts ROCO<sub>2</sub>Li in this study, taking into account the slight shift towards lower BE values due to Na, since those two alkaline cations bring no peaks in the valence spectrum in the 0–27 eV region. Those results in mind, the valence spectra of the HC electrodes obtained after cycling without and with 3% FEC (Figs. 4a and 4b, respectively) can be interpreted as follows: (*i*) First, peak G is only a shoulder on the lower BE side of peak H, which shows that the main carbonaceous species at the surface of the electrodes is ROCO<sub>2</sub>Na and not Na<sub>2</sub>CO<sub>3</sub>. This conclusion is in good agreement with their C 1s spectra in Figs. 3a and 3b. Indeed, for Na<sub>2</sub>CO<sub>3</sub> only one CO<sub>3</sub> component is expected, while for ROCO<sub>2</sub>Na the CO<sub>3</sub> component is accompanied by a C–O component of equal intensity due to R–O group.<sup>34</sup> Actually, due to other minor organic species also present in the SEI, like RONa or poly(ethylene oxide), resulting from solvent degradation at the surface of the HC electrodes, the C–O component is greater than the CO<sub>3</sub> component in the C 1s spectra of the HC

electrodes. (*ii*) Secondly, peaks E and F show that a sodium alkyl carbonate ROCO<sub>2</sub>Na with a R group containing two carbon atoms is the major product. Since lithium ethyl carbonate C<sub>2</sub>H<sub>5</sub>OCO<sub>2</sub>Li (LEC) and lithium ethylene dicarbonate LiO<sub>2</sub>CO–C<sub>2</sub>H<sub>4</sub>–OCO<sub>2</sub>Li (LEDC) have similar valence spectra,<sup>34</sup> and LEDC is usually reported as the main degradation product of EC entering the composition of the SEI in lithium batteries, it can reasonably be assumed that the shape of valence spectra of our HC electrodes can be interpreted by the presence of sodium ethylene dicarbonate NaO<sub>2</sub>CO–C<sub>2</sub>H<sub>4</sub>–OCO<sub>2</sub>Na (NEDC) as the major carbonaceous species of the SEI, resulting from EC decomposition, with or without FEC. This is also in good agreement with previous papers dealing with SEI formation mechanisms related to DMC and EC solvents in sodium cells.<sup>20,35</sup> Finally, a small difference on the valence spectra is observed between the samples cycled without and with 3% FEC, namely the shoulder B at about 8 eV, which is due to NaF. This is in perfect agreement with the previous analysis of F 1s spectra in Fig. 3c showing that the amount of NaF increased 10 times with addition of FEC. The amount of NEDC can be estimated from the intensity of the CO<sub>3</sub> component in C 1s spectra and is found to be about 45 at% without FEC and about 30 at% with 3% FEC, the decrease being mainly due to the increase of aliphatic chains and NaF. While it may have been expected that decomposition mechanism of FEC would lead to the presence additional organic compounds in the SEI, such as polycarbonates or more Na<sub>2</sub>CO<sub>3</sub>, this is not observed here, in good agreement with the study Dahbi et al. over the first cycle.<sup>22</sup> In our case, we observe an increase of the NaF content, but their study was done over the first cycle only, while our study is carried out after long-term cycling. Certainly, the chemical composition of the SEI is not the only reason why the electrochemical behaviour of HC electrodes is better with FEC, but also its thickness and porosity may play a role. While these cannot be probed by XPS, the thickness seems to be in both cases (with and

without FEC) larger than 16–17 nm, which is the estimated probe depth for the higher photon energy used in this work.

**Cycling with NaTFSI salt and FEC additive.**—Figure 5 represents C 1s and F 1s XPS spectra of HC electrodes after 135 cycles in half-cells with NaTFSI/EC:DMC electrolyte, without and with 3% FEC, in the same conditions as previous samples cycled with NaPF<sub>6</sub> salt. Figures depicting other spectra (O 1s, S 2p, Na 2s and N 1s) and the quantification of all peaks are provided in the SI (Fig. S3 and Table SII). When cycling without FEC (upper part of Fig. 5a), results are comparable to those achieved for electrodes cycled with NaPF<sub>6</sub>: the C 1s spectrum is very similar, except for the presence of an additional CF<sub>3</sub> component at 293 eV (light blue) due to TFSI<sup>-</sup> anions. Note that the K 2p<sub>3/2-1/2</sub> signal of potassium (0.4 at% of the surface) is also present on the same spectrum, due to an impurity contained in the salt. Analogous results are achieved for a twice greater probe depth ( $h\nu = 2984.2$  eV, upper part of Fig. 5b). The relative contributions of C–O, COO and CO<sub>3</sub> components are not changed as compared to  $h\nu = 1486.6$  eV photon energy, which indicates that the SEI composition in carbonaceous species is homogeneous over the first 16–17 nm layer. Note that the contribution of NaTFSI salt increases, showing that the remaining salt is not only located at the outermost surface, but also present in deeper layers. As a result, the potassium impurity also increases slightly. As deduced from the F 1s spectrum of the same sample (upper part of Fig. 5c), NaF seems to be present in the SEI (measured amount = 1.2 at%) resulting from salt decomposition. Besides, NaTFSI represents 9 at% of the surface composition of the electrode.

The addition of FEC to NaTFSI based electrolytes induces relevant differences in the spectra of the HC electrodes recovered after cycling, as shown in the bottom part of Fig. 5a. The relative contributions of C–O, COO and CO<sub>3</sub> components in C 1s spectrum are significantly modified. The intensity of the CO<sub>3</sub> component is now greater than the contribution of C–O, indicating that Na<sub>2</sub>CO<sub>3</sub> is present at the surface, which is also confirmed by the lower BE of the CO<sub>3</sub> component (289.5 eV instead of 290.0 eV). Indeed, due to the strong electropositive character of Na, and because the CO<sub>3</sub> group is surrounded by more sodium ions in Na<sub>2</sub>CO<sub>3</sub> than in ROCO<sub>2</sub>Na, the CO<sub>3</sub> component is shifted to lower BE values. The presence of Na<sub>2</sub>CO<sub>3</sub> is consistent with the analysis of the valence spectra of this sample (see below). For the C–C/C–H components, the same trends are observed for electrodes cycled with NaTFSI as those mentioned above for NaPF<sub>6</sub>. Aliphatic chains are present in the SEI, and their amount increases (from 13 to 25 at%) after addition of

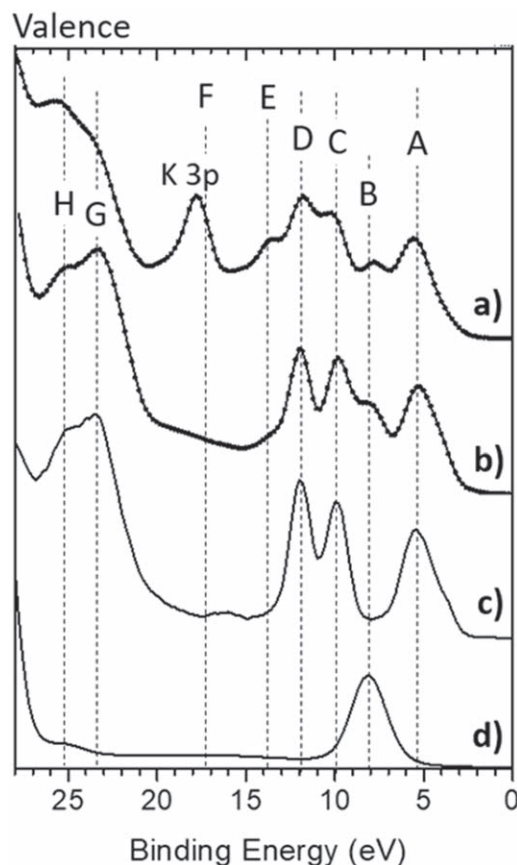


**Figure 6.** XPS valence spectra ( $h\nu = 1487$  eV) of HC electrode after 135 cycles in half-cells with NaTFSI/EC:DMC electrolyte: (a) without FEC, (b) with 3% FEC, compared with valence spectra of: (c) Na<sub>2</sub>CO<sub>3</sub>, (d) NaF.

3% FEC. The peak at low BE in Fig. 5a (purple, 283.5 eV) is attributed to the HC active material surface. This attribution is confirmed by using the higher photon energy 2984.2 eV (leading to a twice greater probe depth, Fig. 5b). Indeed, at this photon energy the C 1s signal of the HC is multiplied by two, which means that the thickness of the SEI is about the same order of magnitude as the probe depth obtained at 1486.6 eV, i.e. 8–9 nm. In the case of

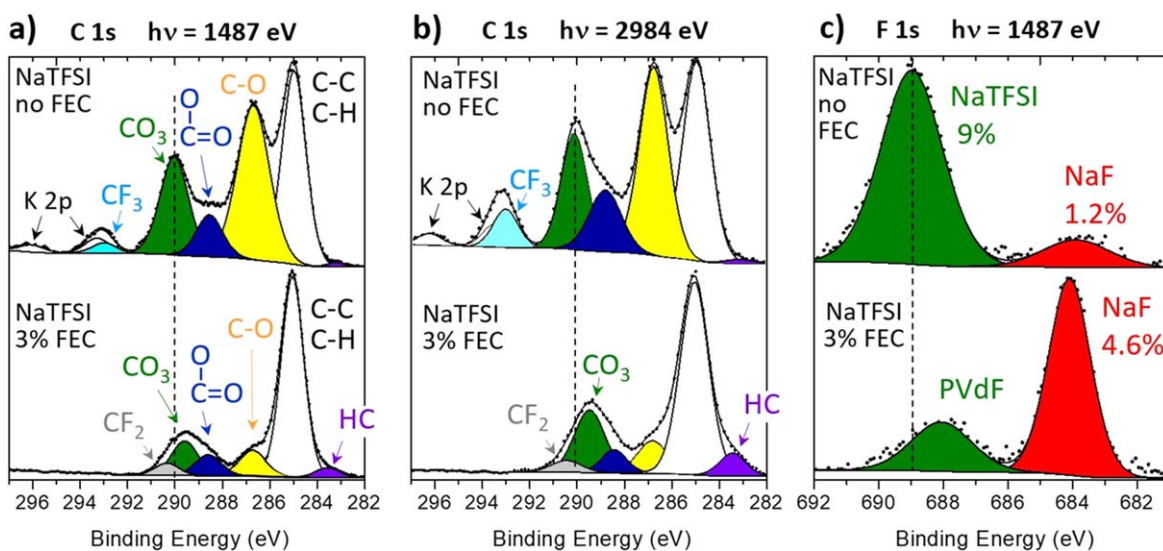


**Figure 5.** (a), (b) C 1s and (c) F 1s XPS spectra of HC electrodes after long cycling in half-cells with NaTFSI/EC:DMC electrolyte, without and with 3% FEC (135 cycles without FEC and 106 cycles with FEC). For C 1s spectra two different photon energies have been used (1487 and 2984 eV, corresponding to two different probe depths).

electrodes cycled in NaTFSI based electrolytes, the presence of FEC leads therefore to a decrease of the SEI thickness. As a result, the  $\text{CF}_2$  signal of the polymer binder PVdF can be simultaneously detected in the C 1s spectrum (grey component at 290.5 eV, with the  $\text{CH}_2$  component of PVdF being included in the yellow component labelled C–O), and also in the F 1s spectrum in Fig. 5c (green component at 688 eV). Moreover, the presence of FEC also results in a significant increase of the NaF amount (4.6 at%).

The XPS valence spectra, for samples cycled with and without FEC are depicted in Fig. 6 and compared with spectra of  $\text{Na}_2\text{CO}_3$  and NaF as reference compounds. The valence spectrum of the HC electrode cycled with 3% FEC (Fig. 6b) is consistent with a simple superposition of the spectra of  $\text{Na}_2\text{CO}_3$  and NaF (6c and 6d), confirming that the SEI composition is dominated by these two species. The valence spectrum of the sample cycled without FEC (Fig. 6a) is very different, the inversion of intensity between peaks G and H revealing the presence of a sodium alkyl carbonate. Unfortunately, the presence of potassium precludes further analysis of 13–20 eV BE, which would otherwise have been relevant,<sup>34</sup> for the attribution of the  $\text{ROCO}_2\text{Na}$  nature. Since peak E can still be recognized and except for the presence of K 3p peak, the spectrum is very similar to its  $\text{NaPF}_6$  counterpart (Fig. 4a) and considering that C 1s spectra of HC electrodes cycled without additive are very similar for  $\text{NaPF}_6$  and NaTFSI, it can be reasonably assumed that the main carbonaceous compound formed in the SEI with NaTFSI without FEC is also  $\text{NaO}_2\text{CO-C}_2\text{H}_4\text{-OCO}_2\text{Na}$  (NEDC). Again, it is possible to estimate the amount of NEDC from the intensity of the  $\text{CO}_3$  component in C 1s spectrum of Fig. 5a: about 45 at% without FEC. As a conclusion, the chemical composition of the organic part of the SEI is not significantly different between NaTFSI and  $\text{NaPF}_6$  based electrolytes when no additive is used but the addition of FEC has a significant influence on it leading to an SEI mainly composed of  $\text{Na}_2\text{CO}_3$  and NaF. The quantitative analysis of core peaks leads to 33 at% of  $\text{Na}_2\text{CO}_3$  and 4.6 at% of NaF, values in good agreement with Carboni et al.<sup>36</sup> who observed  $\text{Na}_2\text{CO}_3$  and NaF as major products deposited at the surface of HC electrodes over 20 cycles when using NaTFSI in PC as electrolyte with FEC additive.

*Cycling with  $\text{NaPF}_6$  or NaTFSI salt and DMCF additive.*—C 1s and F 1s spectra of HC electrodes after 135 cycles with  $\text{NaPF}_6/\text{EC}:\text{DMC}$  electrolyte, without and with 3% DMCF additive, are plotted in Fig. 7. Figures depicting other spectra (O 1s, P 2p and Na 2s) are given in the SI (Fig. S4). The C 1s spectrum without additive in the upper part of Fig. 7a was already presented in Fig. 3a. When using 3% DMCF (bottom part of Fig. 7a), the chemical

composition in carbonaceous species changes significantly with the C 1s spectrum being dominated by a strong  $\text{CO}_3$  component. Taking into account the shift towards lower BE of this component compared to the spectrum without additive, and the very low intensity of the C–O component, this is a clear proof for the presence of a larger amount of  $\text{Na}_2\text{CO}_3$  at the surface. Quantitative analysis from all XPS core peaks revealed indeed the SEI was composed of 75 at% of  $\text{Na}_2\text{CO}_3$  and 5.7 at% of NaF. Contrary to HC electrodes cycled with FEC, the intensity of the C–C, C–H peak is rather low and drops dramatically when the probe depth is increased, indicating that this peak is mainly due to hydrocarbon contamination and not to aliphatic chains. Therefore, the addition of DMCF seems to also lead to a decrease of polyolefin-like species. The analysis of valence spectra, although disturbed by the presence of a potassium impurity of unknown origin (see supplementary information in Fig. S5) confirmed the predominance of  $\text{Na}_2\text{CO}_3$  in the SEI. Increasing the probe depth ( $h\nu = 2984.2$  eV, Fig. 7b) resulted in an important decrease of the K 2p intensity, which is consistent with the location of the potassium impurity at the outermost surface of the sample.

Results corresponding to an analogous study carried out with NaTFSI is presented in Fig. 8, with conclusions being very similar. Indeed, the composition of the SEI changed dramatically with addition of DMCF, with the formation of a larger amount of  $\text{Na}_2\text{CO}_3$  inferred by an intense  $\text{CO}_3$  component correlated to a weak C–O component (Fig. 8a). This is consistent with the valence spectrum, which was only poorly disturbed by a weak amount of potassium (see supplementary information, Fig. S5). The F 1s spectrum revealed the presence of a large amount of NaF. Finally, quantitative analysis allowed to determine the composition of the SEI as 66 at% of  $\text{Na}_2\text{CO}_3$  and 15 at% of NaF. Figures depicting other spectra (O 1s, S 2p, Na 2s and N 1s) are given in the SI (Fig. S6).

As a conclusion, for both salts, the presence of DMCF leads to a massive production of  $\text{Na}_2\text{CO}_3$  with the formation of a rather thick SEI (no trace of HC active material can be detected at  $h\nu = 2984.2$  eV).

**Discussion.**—Overall, the best electrochemical performances achieved in this study were obtained using  $\text{NaPF}_6$  as a salt and FEC (3wt%) as an additive. For such electrolyte formulation the SEI was found to contain mostly NEDC and NaF, from which NEDC is most likely the principal  $\text{Na}^+$  conducting species. However, NEDC rich passivation layer obtained in NaTFSI or  $\text{NaPF}_6$  in EC:DMC electrolytes without additive presented poor capacity retention upon cycling. While NaF is not expected to play a significant role in  $\text{Na}^+$

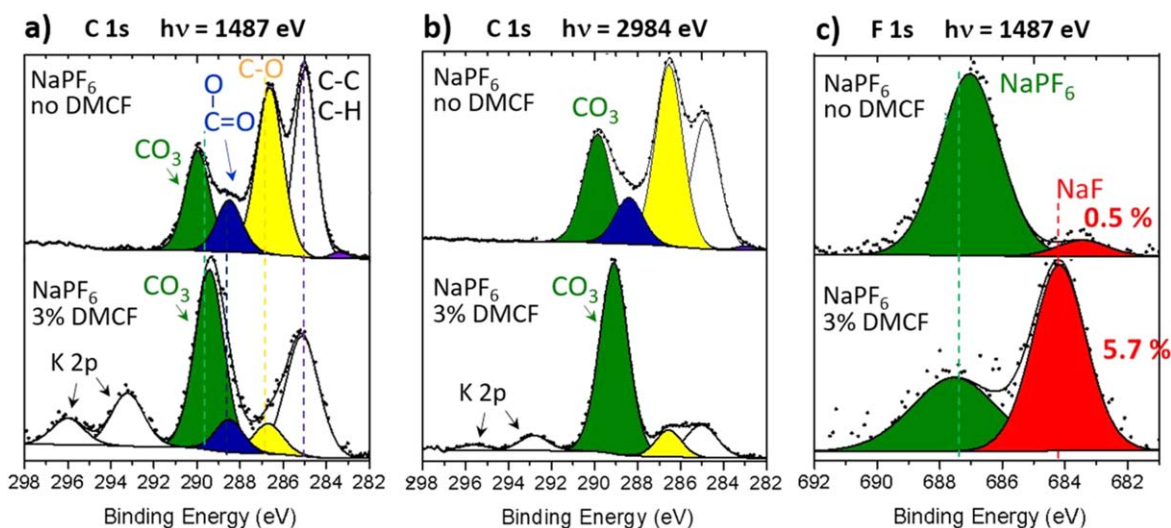


**Figure 7.** (a), (b) C 1s and (c) F 1s XPS spectra of HC electrodes after 135 cycles in half-cells with  $\text{NaPF}_6/\text{EC}:\text{DMC}$  electrolyte, without and with 3% DMCF. For C 1s spectra two different photon energies have been used (1487 and 2984 eV, corresponding to different probe depths).

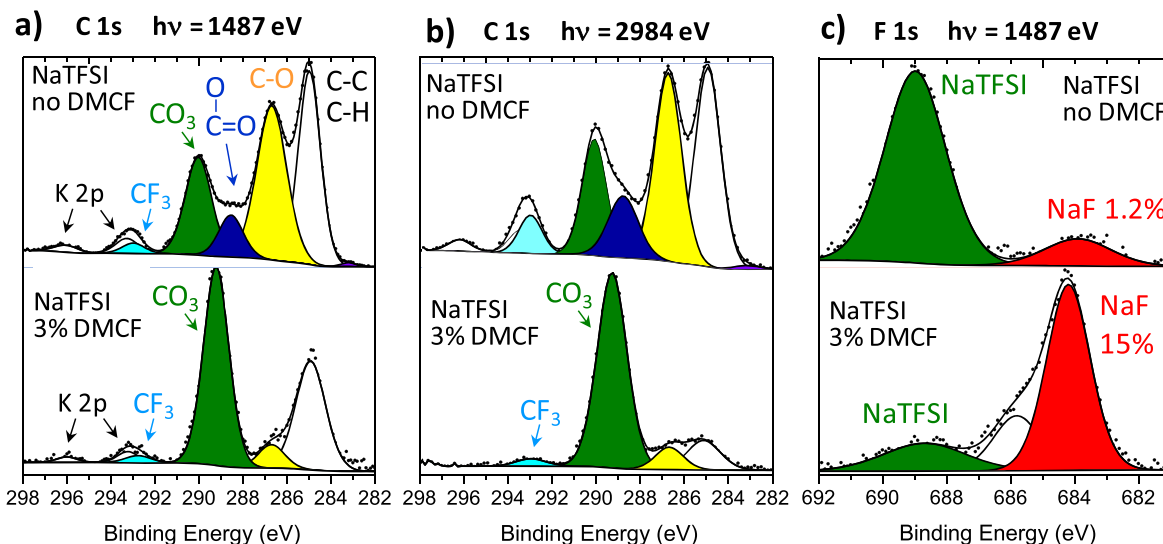


**Figure 8.** (a), (b) C 1s and (c) F 1s XPS spectra of HC electrodes after 135 cycles in half-cells with NaTFSI/EC:DMC electrolyte, without and with 3% DMCF. For C 1s spectra two different photon energies have been used (1487 and 2984 eV, corresponding to different probe depths).

migration through the SEI since it is even less conducting than its Li analog, LiF,<sup>37</sup> a significant improvement in terms of capacity retention was observed in NaPF<sub>6</sub> potentially related to the increase in the amount of NaF in the SEI through the addition of FEC (respectively, 0.5 and 5.5% of NaF, without and with FEC). Indeed, and in the conditions evaluated in this work, NaF content in the SEI > 4% appeared to be the common denominator for high capacity retention tests (all tests performed with DMCF and FEC). While the role of NaF remains unclear and other parameters such as porosity, thickness and homogeneity of the SEI should be carefully investigated, it is interesting to note that the presence of a presumably “bad” SEI component such as NaF can play a beneficial role in the electrochemical performances of hard carbon electrodes. We tentatively rationalized these results by considering that the SEI must play one major role aside from being electronically insulating and ionically conducting, which is to be stable (or insoluble). As mentioned before this is not obvious in Na cells as most Na salts tend to be more soluble than their Li analogs.<sup>16</sup> Such potential SEI solubility issue can play an important role in interfacial processes since a partially dissolved SEI will result in continuous electrolyte decomposition and capacity fading. Hence, the presence of a rather insoluble species such as NaF can play an important role in stabilizing the SEI and in limiting solubility issues related to other compounds (such as NEDC here). Interestingly, recent studies on Li-ion counterparts have shown that the presence of LiF has also a positive impact on the electrochemical performances, the key point being to understand how LiF is distributed in the SEI,<sup>38</sup> and hence a similar effect can be expected for Na-ion batteries. While, the beneficial role of NaF on capacity retention is evidenced in this work, the determination of the optimal SEI composition leading to high overall capacity is not trivial. For instance, samples with similar amount of NaF present significant difference in capacities (such as NaPF<sub>6</sub> + 3% FEC or +3% DMCF, both with 5.5%–5.7% of NaF). Other parameter affecting the capacity should thus be considered. Another aspect which has been suggested to be beneficial for Li-ion cells is the composite nature of the passivation layer, as the presence of multiple grain boundaries may promote space charge accumulation and boost ionic conduction.<sup>39</sup> While this phenomenon could lead to lower polarization and thus higher capacity, it is expected that the way SEI components are mixed together will play an important role.

## Conclusions

The influence of two salts (NaPF<sub>6</sub>, NaTFSI) and two additives (FEC, DMCF) on the electrochemical behavior of HC//Na half-cells over long-term cycling (135 cycles) is reported, performance being better with NaPF<sub>6</sub> than with NaTFSI. With NaPF<sub>6</sub>, the use of 3% FEC improves significantly the overall capacity as well as capacity retention, whereas the use of DMCF additive has a detrimental effect on capacity but resulted in better cyclability than with additive free electrolyte. With NaTFSI, both additives have a beneficial effect, although the electrochemical behavior is not as good as with NaPF<sub>6</sub> salt. Chemical characterization of the HC electrode’s surface by XPS has shown that the SEI composition is mainly composed of sodium ethylene dicarbonate NaO<sub>2</sub>CO-C<sub>2</sub>H<sub>4</sub>-OCO<sub>2</sub>Na (NEDC) and NaF for the best electrochemical performances (with NaPF<sub>6</sub> and 3%FEC) over 135 cycles. The use of FEC together with NaTFSI, or DMCF with both salts, leads to an SEI mainly composed of Na<sub>2</sub>CO<sub>3</sub> and NaF, with poorer electrochemical performances. This suggests that the presence of NEDC has a beneficial role in physical/chemical properties of the SEI. For NEDC rich SEI the presence of NaF (enhanced when using FEC as additive) was found to significantly improve the capacity retention upon cycling. This was tentatively ascribed to a beneficial role of the NaF in limiting the solubility of NEDC or to an improved Na<sup>+</sup> conduction through the SEI due to space charge accumulation. Unfortunately, no direct conclusions could be made on the parameters affecting the overall capacity and future work should also consider parameters such as the SEI morphology or thickness. This study gives a complementary view of the SEI chemistry of Na-ion batteries after long-term cycling, as a complement to previous studies dealing with the first cycles. A SEI engineering strategy based in the incorporation of highly insoluble species may be useful to mitigate solubility issues and improve cycle life.

## Acknowledgments

Authors acknowledge the European Commission for funding through H2020 NAIADES project (LCE10–2014, grant nb. 646433). EI, MRP and AP acknowledge Ministerio de Economía y Competitividad (Spain) for Severo Ochoa Programme for Centres of Excellence in R&D (SEV-2015-0496). This work has been done in the frame of the Doctoral Degree Program in Chemistry by the Universitat Autònoma de Barcelona. JF, CC and RD acknowledge Agence Nationale de la Recherche (ANR) for its “Investment for the Future” Program through I-SITE E2S-UPPA funding.

## ORCID

M. R. Palacin  <https://orcid.org/0000-0001-7351-2005>A. Ponrouch  <https://orcid.org/0000-0002-8232-6324>

## References

1. E. A. Olivetti, G. Ceder, G. G. Gaustad, and X. Fu, "Lithium-ion battery supply chain considerations: analysis of potential bottlenecks in critical metals." *Joule*, **1**, 229 (2017).
2. N. Yabuuchi, K. Kubota, M. Dahbi, and S. Komaba, "Research development on Sodium-Ion batteries." *Chem. Rev.*, **114**, 11636 (2014).
3. P. Johansson, P. Rozier, and M. R. Palacin, "Na-ion batteries." in *Prospects for Li-ion Batteries and Emerging Energy Electrochemical Systems*, ed. L. Croguennec and L. Monconduit (World Scientific Europe, Singapore)161 (2018), Series on Chemistry, Energy and the Environment, Book 4, Chap. 4, p.
4. E. J. Berg, C. Villeveuille, D. Streich, S. Trabesinger, and P. Novák, "Rechargeable batteries: grasping for the limits of chemistry." *J. Electrochem. Soc.*, **162**, A2468 (2015).
5. C. Vaalma, D. Buchholz, M. Weil, and S. Passerini, "A cost and resource analysis of Sodium-Ion batteries." *Nature Reviews Materials*, **3**, 18013 (2018).
6. J. Peters, D. Buchholz, S. Passerini, and M. Weil, "Life cycle assessment of Sodium-Ion batteries." *Energy Environ. Sci.*, **9**, 1744 (2016).
7. E. Irisarri, A. Ponrouch, and M. R. Palacin, "Review - hard carbon negative electrode materials for Sodium-Ion batteries." *J. Electrochem. Soc.*, **162**, A2476 (2015).
8. R. Dugas, B. Zhang, P. Rozier, and J. M. Tarascon, "Optimization of Na-Ion battery systems based on polyanionic or layered positive electrodes and carbon anodes." *J. Electrochem. Soc.*, **163**, A867 (2016).
9. A. Ponrouch, D. Monti, A. Boschini, B. Steen, P. Johansson, and M. R. Palacin, "Non-aqueous electrolytes for Sodium-Ion batteries." *J. Mater. Chem. A*, **3**, 22 (2015).
10. E. Peled, "The electrochemical behavior of Alkali and Alkaline earth metals in nonaqueous battery systems - the solid electrolyte interphase model." *J. Electrochem. Soc.*, **126**, 2047 (1979).
11. R. Mogensen, D. Brandell, and R. Younesi, "Solubility of the solid electrolyte interphase (SEI) in sodium ion batteries." *ACS Energy Lett.*, **1**, 1173 (2016).
12. K. Xu, "Nonaqueous liquid electrolytes for lithium-based rechargeable batteries." *Chem. Rev.*, **104**, 4303 (2004).
13. K. Xu, "Electrolytes and Interphases in Li-Ion batteries and beyond." *Chem. Rev.*, **114**, 11503 (2014).
14. S. K. Heiskanen, J. Kim, and B. L. Lucht, "Generation and evolution of the solid electrolyte interphase of Lithium-Ion batteries." *Joule*, **3**, 2322 (2019).
15. J. Song, B. Xiao, Y. Lin, K. Xu, and X. Li, "Interphases in Sodium-Ion batteries." *Adv. Energy Mater.*, **8**, 1703082 (2018).
16. D. I. Iermakova, R. Dugas, M. R. Palacin, and A. Ponrouch, "On the comparative stability of Li and Na metal anode interfaces in conventional Alkyl carbonate electrolytes." *J. Electrochem. Soc.*, **162**, A7060 (2015).
17. L. Schafzahl, H. Ehmman, M. Kriechbaum, J. Sattelkow, T. Ganner, H. Plank, M. Wilkening, and A. Freunberger, "Long-chain Li and Na Alkyl carbonates as solid electrolyte interphase components: structure, ion transport, and mechanical properties." *Chem. Mater.*, **30**, 3338 (2018).
18. G. G. Eshetu, S. Grugeon, H. Kim, S. Jeong, L. Wu, G. Gachot, S. Laruelle, M. Armand, and S. Passerini, "Comprehensive insights into the reactivity of electrolytes based on sodium ions." *ChemSusChem*, **9**, 462 (2016).
19. A. Ponrouch, R. Dedryvère, D. Monti, J. M. Ateba Mba, L. Croguennec, C. Masquelier, P. Johansson, and M. R. Palacin, "Towards high energy density sodium ion batteries through electrolyte optimization." *Energy Environ. Sci.*, **6**, 2361 (2013).
20. Y. Pan, Y. Zhang, B. S. Parimalam, C. C. Nguyen, G. Wang, and B. L. Lucht, "Investigation of the solid electrolyte interphase on hard carbon electrode for sodium ion batteries." *J. Electroanalytical Chem.*, **799**, 181 (2017).
21. S. Komaba, T. Ishikawa, N. Yabuuchi, W. Murata, A. Ito, and Y. Ohsawa, "Fluorinated ethylene carbonate as electrolyte additive for rechargeable Na batteries." *ACS Appl. Mater. Interfaces*, **3**, 4165 (2011).
22. M. Dahbi, T. Nakano, N. Yabuuchi, S. Fujimura, K. Chihara, K. Kubota, J. Y. Son, Y. T. Cui, H. Oji, and S. Komaba, "Effect of Hexafluorophosphate and Fluoroethylene carbonate on electrochemical performance and the surface layer of hard carbon for Sodium-Ion batteries." *ChemElectroChem*, **3**, 1856 (2016).
23. E. de la Llave, V. Borgel, E. Zinigrad, F. F. Chesneau, P. Hartmann, Y. K. Sun, and D. Aurbach, "Study of the most relevant aspects related to hard carbons as anode materials for Na-ion batteries, compared with Li-ion systems." *Isr. J. Chem.*, **55**, 1260 (2015).
24. A. Bouibes, N. Takenaka, T. Fujie, K. Kubota, S. Komaba, and M. Nagaoka, "Concentration effect of Fluoroethylene carbonate on the formation of solid electrolyte interphase layer in Sodium-Ion batteries." *ACS Appl. Mater. Interfaces*, **10**, 28585 (2018).
25. A. Ponrouch, A. R. Goñi, and M. R. Palacin, "High capacity hard carbon anodes for sodium ion batteries in additive free electrolyte." *Electrochem. Comm.*, **27**, 85 (2013).
26. R. Dugas, A. Ponrouch, G. Gachot, R. David, M. R. Palacin, and J.-M. Tarascon, "Na Reactivity toward Carbonate-based electrolytes: the effect of FEC as additive." *J. Electrochem. Soc.*, **163**, A2333 (2016).
27. B. Garcia and M. Armand, "Aluminium corrosion in room temperature molten salt." *J. Power Sources*, **132**, 206 (2004).
28. D. A. Stevens and J. R. Dahn, "The mechanisms of Lithium and Sodium insertion in carbon materials." *J. Electrochem. Soc.*, **148**, A803 (2001).
29. C. Bommier, T. W. Surta, M. Dolgos, and X. Ji, "New mechanistic insights on Na-Ion storage in nongraphitizable carbon." *Nano Lett.*, **15**, 5888 (2015).
30. A. Ponrouch and M. R. Palacin, "On the high and low temperature performances of Na-ion battery materials: hard carbon as a case study." *Electrochem. Comm.*, **54**, 51 (2015).
31. S. Tanuma, C. J. Powell, and D. R. Penn, "Calculations of electron inelastic mean free paths. IX. Data for 41 elemental solids over the 50 eV to 30 keV range." *Surf. Interface Anal.*, **43**, 689 (2011).
32. R. Dedryvère, S. Laruelle, S. Grugeon, P. Poizat, D. Gonbeau, and J.-M. Tarascon, *Chem. Mater.*, **16**, 1056 (2004).
33. D. Aurbach, B. Markovsky, I. Weissman, E. Levi, and Y. Ein-Eli, *Electrochim. Acta*, **45**, 67 (1999).
34. R. Dedryvère, L. Gireaud, S. Grugeon, S. Laruelle, J.-M. Tarascon, and D. Gonbeau, *J. Phys. Chem. B*, **109**, 15868 (2005).
35. G. Yan, D. Alves-Dalla-Corte, W. Yin, N. Madern, G. Gachot, and J.-M. Tarascon, "Assessment of the electrochemical stability of Carbonate-based electrolytes in Na-ion batteries." *J. Electrochem. Soc.*, **165**, A1222 (2018).
36. M. Carboni, J. Manzi, A. R. Armstrong, J. Billaud, S. Brutti, and R. Younesi, "Analysis of the solid electrolyte interphase on hard carbon electrodes in Sodium-ion batteries." *ChemElectroChem*, **6**, 1745 (2019).
37. H. Yildirim, A. Kinaci, M. K. Y. Chan, and J. P. Greeley, "First-principles analysis of defect thermodynamics and Ion transport in inorganic SEI compounds: LiF and NaF." *ACS Appl. Mater. Interfaces*, **7**, 18985 (2015).
38. C. Wang, Y. S. Meng, and K. Xu, "Fluorinating interphases." *J. Electrochem. Soc.*, **166**, A5184 (2019).
39. Q. Zhang, J. Pan, P. Lu, Z. Liu, M. W. Verbrugge, B. W. Sheldon, Y.-T. Cheng, Y. Qi, and X. Xiao, "Synergetic effects of inorganic components in solid electrolyte interphase on high cycle efficiency of Lithium Ion batteries." *Nano Lett.*, **16**, 2011 (2016).